

Energy Reserves and Clearing in Stochastic Power Markets: The Case of Plug-In-Hybrid Electric Vehicle Battery Charging

Justin M. Foster, *Student Member, IEEE*, and Michael C. Caramanis, *Member, IEEE*

Abstract—Building on our previous work in plug-in-hybrid electric vehicle (PHEV) charging, we study the potential benefits of demand participating in precisely quantified quality of service trades. Given the equivalency of demand and generation modulation in effecting power system cost and stability, we consider demand and generation as market participants with equal rights who engage in a mix of energy and reserve market transactions that clear simultaneously. Using existing market practice in the clearing of energy and reserves, we formulate the optimal bidding strategy of a load aggregator responsible for the battery charging of a fleet of PHEVs as the solution to a stochastic dynamic program (SDP). We show that optimal PHEV energy and regulation service bids lower PHEV charging costs, mitigate local distribution network congestion constraints, and increase system-wide supply of regulation service and thus contribute to the efficient expansion of intermittent clean generation. We propose and implement a tractable approximate SDP solution and report on computational experience using ERCOT and CAISO data.

I. INTRODUCTION

The burden of intermittent renewable generation on power system security and stability costs has been a topic of increasing debate over the past decade [14], [22]. The inability to dispatch wind generation and its variability over time-scales of minutes are likely to increase the reserves required to safeguard system stability including regulation service (5 minute time-scale) and operating reserves (10 minute time-scale). Consequently, although wind energy can be generated at competitive prices, large-scale adoption may place a costly burden on regulation service reserves. Currently, such reserves are provided by flexible generation; however, we argue that efficient load-side provided reserves can help mitigate this problem.

A. Wind Generation Integration

Recent studies as well as empirical evidence [6], [7], [12], [13] indicate that the increased market penetration of wind generation will result in significant increases in regulation service reserve requirements. Although preliminary reports by the California Energy Commission in 2007 [18] concluded only modest increases in regulation service due to substantial wind generation expansion, in 2009, Makarov et al. [12] reported that for a 4,100 MW increment of wind farm nameplate capacity in California, a maximum increase

of 230 MW (5.6%) of regulation-service-down and 500 MW (12.2%) of regulation-service-up would be required. In addition, areas with high wind penetration have experienced sudden losses of wind power. In Texas, ERCOT reported wind output during certain hours in 2007 that was 2,000 MW short of the forecast while in 2008 wind output unexpectedly dropped 1,300 MW in three hours [6]. In Europe (e.g., Spain), similar system stability issues due to wind have been experienced [4], [7].

B. PHEV Charging Synergies

Significant adoption of wind generation could increase regulation service clearing prices which today fall in the \$10-\$60 per MWh range. Thus, under a business-as-usual scenario, regulation service costs may pose a serious barrier to renewable generation expansion. However, since generation and demand will be market participants with equal rights, it is of paramount importance to investigate demand-side contributions that ease the price pressure on reserve procurement. This paper does exactly this by proposing a decision support algorithm for optimal PHEV market bidding that promises to realize the technical capabilities of PHEV loads [9], [10]. Furthermore, since PHEV charging will draw power from the distribution network, we incorporate local distribution congestion [2], [11] in the optimal PHEV market bidding strategies. Implementation of our algorithm using ERCOT and CAISO data shows strong positive synergies between wind generation and flexible PHEV loads.

C. Power Market Structure and Participation Rules

Smith et al. stated that “operating experience from around the world has shown that a deep, liquid, real-time market is the most economical approach to providing the balancing energy required by variable-output wind plants [22].” In the US, day-ahead, adjustment, and real-time power markets have been operating since the mid 1990s (i.e., CAISO, ERCOT, MISO, PJM, NEISO, NYISO, and SPP). As a result of FERC Order 719, each independent system operator has a demand response program in some stage of development. For example, PJM has allowed demand response by end-use customers, through curtailment service providers, to participate alongside generation in offering capacity reserves to the market since 2006 [17], [19]. At around the same time NEISO implemented Real-Time Price Response and Day-Ahead Load Response Programs. The NYISO has four demand response programs, including a Demand-Side Ancillary Services Program. The CAISO will

Both authors are with the Division of Systems Engineering, Boston University College of Engineering, Boston MA, e-mail: jfoster2@bu.edu and mcaraman@bu.edu. Research reported here has been supported by an EPA STAR Fellowship, Switzer Fellowship, and NSF IGERT.

begin in 2010 to offer a Proxy Demand Response product, which is a load or aggregation of loads that can submit bids into the wholesale day-ahead and real-time markets and respond to dispatches at the direction of the CAISO.

In this paper, we assume a power market structure similar to those currently existing in the US, but allowing for symmetry in the generation- and load-side participation, which we assume will become feasible with the advent of the SmartGrid [9]. In particular, for each scheduling period, t , supply- and demand-side market participants submit bids for energy. In addition, they make capacity reserve offers for primary, secondary (regulation service), and tertiary (operating) reserves. Primary, regulation service, and operating reserve offers represent standby capacity that must be deliverable in 30 sec, 5 min, and 15 min, respectively. Primary and secondary reserves must respond to frequency tolerances and centralized control commands to maintain the market's real-time energy balance. Moreover, they involve a symmetric band of up-and-down capacity (i.e., increment or decrement) in the amount of capacity offered. Hence frequency control and regulation service reserve bids include an *energy* and a *capacity standby* price.

To elaborate by example, consider a Load Aggregator or Energy Service Company (ESCO) purchasing energy and offering regulation service in decision period t . For the energy bid, the ESCO submits a quantity (or rate KW) and a price bid (\$ per KWh),

$$Q_t^E \text{ and } u_t^E.$$

The regulation service bid consists of a quantity and two prices,

$$Q_t^R, u_t^{RE}, \text{ and } u_t^{RC}.$$

Again, the two prices included in the regulation service bid correspond respectively to the energy reservation price and the cost of modulating consumption (or generation) in real-time to respond to centralized control commands. For example, if an ESCO is scheduled by the clearing of the market to provide regulation service it will (i) start the period consuming at the rate of Q_t^R and be charged at the market energy clearing price; (ii) be credited at the market regulation service clearing price; and (iii) respond to market operator commands to consume at any level in the interval $[0, 2Q_t^R]$, moving towards the level that the operator indicates at the rate of $Q_t^R/5$ KW per min.

The market operator receives bids and offers from all market participants and clears the market to minimize costs over one (real-time) or more (day-ahead) time period(s). For each period, market-wide prices are obtained and individual participant energy and reserve bids and offers are scheduled. We assume competitive conditions and symmetric availability of information represented by the joint probability distribution (jpd) of clearing prices conditional upon the current state of the system.

The jpd allows each market participant to evaluate the probability of four key events described in (1), (2), (3), and (4). It is important to note that the probability of these events,

$$p_t^k \text{ for } k = e_0, e_1, e_2, e_3,$$

is a function of the bid prices of the market participant. The energy bid is accepted according to (1).

$$\text{Event } e_0 : u_t^E \geq \tilde{P}_t^E \quad (1)$$

The expected cost of the energy bid is the product of the probability of acceptance, the conditional expected clearing price, and the bid quantity,

$$p_t^{e_0} E_{\tilde{P}_t^E} [\tilde{P}_t^E] Q_t^E.$$

The regulation service offer can be accepted (2), rejected but the energy component scheduled (3) or both the regulation service and its energy component can both be rejected (4).

$$\text{Event } e_1 : \left| \tilde{P}_t^E - u_t^{RE} \right| + u_t^{RC} \leq \tilde{P}_t^R \quad (2)$$

$$\text{Event } e_2 : \left| \tilde{P}_t^E - u_t^{RE} \right| + u_t^{RC} > \tilde{P}_t^R \text{ and } u_t^{RE} \geq \tilde{P}_t^E \quad (3)$$

$$\text{Event } e_3 : \left| \tilde{P}_t^E - u_t^{RE} \right| + u_t^{RC} > \tilde{P}_t^R \text{ and } u_t^{RE} < \tilde{P}_t^E \quad (4)$$

Since events e_1 and e_2 are disjoint, the expected cost of the regulation service bid is

$$p_t^{e_1} E_{\tilde{P}_t^E} \left[\tilde{P}_t^E - \tilde{P}_t^R \right] Q_t^R + p_t^{e_2} E_{\tilde{P}_t^R | e_2} \left[\tilde{P}_t^E \right] Q_t^R.$$

D. Day-Ahead, Adjustment, and Real-Time Markets

There are several related short-term markets that clear in the course of a day. The *day-ahead market* closes to bids and offers at noon of the day before the operating day. It schedules simultaneously bids and offers and determines clearing prices for each of the 24 hours in the operating day. This market performs short-term planning (e.g., hedging, unit commitment, reserve scheduling) functions. *Adjustment markets* allow market response to significant events such as major equipment failures or forecast revisions that occur after the day-ahead market closes. They are qualitatively the same as the day-ahead market. The *real-time market* typically closes 45 minutes before time the operating time schedules bids and offers for the next 5, 10, or 15 minutes. It performs the final adjustments when essentially all uncertainty has been realized and feasible operational decisions can be made. Its basic difference from the day-ahead and adjustment markets is that it schedules a *single* as opposed to *multiple* periods.

As we have mentioned, it is reasonable to assume that demand-side market participants will be Load Aggregators or Energy Service Companies (ESCOs) that take advantage of pooling, decision support intelligence, and information gathering. These companies typically have regionally specific names, such as Curtailment Service Providers in PJM and Enrolling Participant in NEISO. For example, an ESCO may be handling PHEVs plugging into outlets on one

or more residential feeders or commercial facilities. The ESCo will participate in the cascaded markets described above, making hedging purchases of energy and sales of regulation service in the day-ahead market with the view that it will be able to adjust in the real-time market. The coupling of decisions in the sequential cascaded markets is considered in [3] where we argue that the main building block for the coordinated decision making across markets is the real-time market. We present next the real-time market problem and propose a tractable solution algorithm.

II. REAL-TIME MARKET SINGLE FEEDER PROBLEM

During each real-time market time period, the ESCo bids for energy and offers regulation service, while charging a fleet of PHEVs. These PHEVs are located in different parts of the distribution network; however, distribution network constraints force us to group the PHEVs according to a specific distribution network capacity (e.g., feeder or transformer capacity). Decisions for all distribution network capacity constraints would be aggregated in order to determine the total bidding policy of the ESCo. We present below the problem of charging a fleet of PHEVs constrained by a single feeder capacity. Although we model a 24 hour horizon, we approximate an infinite horizon by estimating the marginal cost of charging PHEVs plugged-in within the modeled horizon but intending to depart outside the horizon.

A. Indices

- t, Δ_t Market decision period and its duration.
 τ Index of plugged-in PHEV departure classes.

B. Problem Parameters

- N Number of time periods in the finite horizon.
 c Penalty of uncharged energy at time of PHEV departure (\$ per KWh).
 r Charging rate of each PHEV (KW).
 \hat{C}_t^{\max} Feeder specific unused capacity available for PHEV battery charging (KW).
 λ_{N}^{τ} Marginal costs of charging PHEVs with departure class outside of the modeled horizon (i.e., $\tau > N$) (\$ per KWh).

C. State and Decision Variables

- n_t^{τ} Number of PHEVs plugged-in at the beginning of period t , in departure class τ .
 x_t^{τ} Uncharged energy of PHEVs plugged-in at the beginning of period t , in departure class τ (KWh).
 $Q_t^E(\tau)$ Energy rate bid for period decision period t . Intended for charging x_t^{τ} (KW).
 $Q_t^R(\tau)$ Regulation service capacity offered, for decision period t . Intended for charging x_t^{τ} (KW).
 $u_t^E(\tau)$ Energy bid price for $Q_t^E(\tau)$ (\$ per KWh).
 $u_t^{RE}(\tau)$ Energy price offered for $Q_t^R(\tau)$ (\$ per KWh).

- $u_t^{RC}(\tau)$ Capacity price offered for $Q_t^R(\tau)$ (\$ per KWh).
 \mathbf{u}_t A vector containing all decision variables for decision period t .
 \mathbf{I}_t Relevant information or state vector for decision period t . This includes joint probability distributions of future PHEV demand, line capacities, and market clearing prices. In addition, it contains results of cleared markets and up-to-date power system information. Finally, it consists of \hat{C}_t^{\max} , n_t^{τ} , and x_t^{τ} .

D. Random Variables and Density Functions

- E_t Expectation operator.
 \tilde{P}_t^E Real-time market energy clearing price during period t (\$ per KWh).
 \tilde{P}_t^R Real-time market regulation service clearing price during period t (\$ per KWh).
 $\tilde{\Delta}n_t^{\tau}$ Number of PHEVs that plug-in during period t in departure class τ .
 $\tilde{\Delta}x_t^{\tau}$ Uncharged energy of PHEVs that plug-in during period t in departure class τ (KWh).
 $p_t^k(\tau)$ The probability of events $k = e_0, e_1, e_2, e_3$ for bids $Q_t^E(\tau)$ and $Q_t^R(\tau)$.
 $\tilde{I}_E^{\tau}(\mathbf{u}_t)$ Indicator function which takes the value of one if $Q_t^E(\tau)$ is accepted. This occurs with probability $p_t^{e_0}(\tau)$.
 $\tilde{I}_{RS}^{\tau}(\mathbf{u}_t)$ Indicator function which takes the value of one if $Q_t^R(\tau)$ is accepted in some form. This occurs with probability $p_t^{(e_1 \cup e_2)}(\tau)$.

E. System Dynamics

The dynamics of the number of PHEVs plugged-in is presented in (5). Up-and-down reserves, including regulation service, are exercised by the market operator so that over a period of a half hour or longer energy neutrality is maintained; therefore, the uncharged capacity dynamics can be expressed as in (6). Finally, all PHEVs are assumed to un-plug at their scheduled departure time (7).

$$n_{t+1}^{\tau} = n_t^{\tau} + \tilde{\Delta}n_t^{\tau} \quad \forall \tau > t \quad (5)$$

$$x_{t+1}^{\tau} = x_t^{\tau} + \tilde{\Delta}x_t^{\tau} - \left[\tilde{I}_E^{\tau}(\mathbf{u}_t) Q_t^E(\tau) + \tilde{I}_{RS}^{\tau}(\mathbf{u}_t) Q_t^R(\tau) \right] \Delta_t \quad \forall \tau > t \quad (6)$$

$$n_t^{\tau} = x_t^{\tau} = 0 \quad \forall \tau \leq t \quad (7)$$

F. Allowable Decisions

The ESCo must follow market rules to insure that its energy bid and regulation service offer are realizable. This requires that two constraints on the maximal consumption rate (i.e., the requested energy rate plus *twice* the offered regulation service). *First*, the excess feeder capacity should be sufficient to support the maximal consumption rate (8).

Second, there must be enough plugged-in PHEVs to absorb the maximal charging rate (9). Constraint (10) does not allow more energy to be charged than the current uncharged capacity. Note that (8) couples the departure classes. In addition, the allowable control set includes non-negativity constraints on all the state and decision variables.

$$\sum_{\tau} [Q_{\tau}^E(\tau) + 2Q_{\tau}^R(\tau)] \leq \hat{C}_i^{\max} \quad (8)$$

$$Q_{\tau}^E(\tau) + 2Q_{\tau}^R(\tau) \leq m_i^{\tau} \quad \forall \tau > t \quad (9)$$

$$\left[Q_{\tau}^E(\tau) + Q_{\tau}^R(\tau) \right] \Delta_{\tau} \leq x_i^{\tau} \quad \forall \tau > t \quad (10)$$

G. Bellman Equation

Decisions are made for each decision period t based on the available information at the time the market closes. The Bellman Equation is presented in (11).

$$J_t(\mathbf{I}_t) = \min_{\mathbf{u}_t \in U_t(\mathbf{I}_t)} E_t \left[g_t(\mathbf{I}_t, \mathbf{u}_t, \tilde{P}_t^E, \tilde{P}_t^R, t) + J_{t+1}(\mathbf{I}_{t+1}) \right]$$

With boundary condition,

$$J_N(\mathbf{I}_N) = c x_{\tau=N}^{\tau} + \sum_{\tau > N} x_{\tau=N}^{\tau} \lambda_N^{\tau}.$$

Where $E_t \left[g_t(\mathbf{I}_t, \mathbf{u}_t, \tilde{P}_t^E, \tilde{P}_t^R, t) \right] =$ (11)

$$c x_{\tau=\tau}^{\tau} + \sum_{\tau} \left\{ \begin{array}{l} p_t^{e_0}(\tau) E_t \left[\tilde{P}_t^E \right] Q_{\tau}^E(\tau) + \\ p_t^{e_1}(\tau) E_t \left[\tilde{P}_t^E - \tilde{P}_t^R \right] Q_{\tau}^R(\tau) + \\ p_t^{e_2}(\tau) E_t \left[\tilde{P}_t^E \right] Q_{\tau}^R(\tau) \end{array} \right\}$$

III. SOLUTION APPROACH ADOPTED

A full backward recursion solution of the proposed finite horizon SDP problem is not tractable for any real system. In addition to overall complexity, the SDP problem is formidable due to (i) uncountable state and control spaces and (ii) the non-linearity and associated non-convexity introduced by regulation service bid price decisions. In order to deal with the non-convexity issue, we implement a price-takers bidding policy shown in (12)-(14).

$$u_t^E(\tau) \gg E_t \left[\tilde{P}_t^E \right], \quad \forall t, \forall \tau \quad (12)$$

$$u_t^{RE}(\tau) = E_t \left[\tilde{P}_t^E \right], \quad \forall t, \forall \tau \quad (13)$$

$$u_t^{RC}(\tau) = 0, \quad \forall t, \forall \tau \quad (14)$$

As a result, the energy bid is accepted almost certainly, and we maximize the probability the regulation service bid is accepted. In addition, note that the probability of the four key events is now the same for all τ , so we can write,

$$p_t^k(\tau) = p_t^k, \quad \forall t, \forall \tau, \text{ and}$$

$$\tilde{\mathbf{I}}_{\text{RS}}^{\tau}(\mathbf{u}_t) = \tilde{\mathbf{I}}_{\text{RS}}(\mathbf{u}_t), \quad \forall t, \forall \tau.$$

The most significant uncertainty in the state variables is the binary realization of whether each regulation service

offer is accepted or rejected. Therefore, we propose to model the evolution of these uncertainties by implementing a limited look-ahead SDP algorithm that uses a Multistage Stochastic Programming (MSP) formulation [20]. MSP formulations have proved useful in capacity planning [8], [21], as well as power generation scheduling in the day-ahead electricity market [25]. A MSP model approximates the SDP *cost-to-go* with a limited look-ahead that explicitly represents and prepares for many possible states of the system with the objective to minimize expected costs. In addition, the formulation allows for the revision of charging decisions in each time stage based on the uncertainty realized so far (i.e., an optimal open loop feedback formulation). Whereas we replace certain random variables by their expected values (e.g., PHEV demand pattern), we develop the scenario tree based on sequential regulation service bids being accepted or rejected. More precisely, we build the scenario trees based on all possible realizations of $\tilde{\mathbf{I}}_{\text{RS}}(\mathbf{u}_t)$.

The number of state and decision variables for the finite horizon MSP can be computed according to (15). Therefore, the inclusion of all possible scenarios would result in a model of intractable size. As a result, we consider a limited look-ahead for a portion of the horizon combined with a certainty equivalent for the remaining horizon. The scenario tree branches according to the regulation service indicator function at each time period $t = 0, 1, \dots, b$ where b is large enough to capture the benefit of look-ahead while avoiding an intractable number of decision variables. This is a reasonable approach since rejected regulation service offers to charge PHEVs with distant departure times can be compensated for with future bids while bids intended to charge PHEVs whose departure time is close can benefit from the more accurate look-ahead formulation. A similar effort to minimize the number of selected scenarios is included in [25].

$$3 \sum_{i=0}^{N-1} (2N-i) 2^i + N 2^i \quad (15)$$

We denote the scenario tree by \mathcal{T} , and let \mathcal{N} be the set of nodes in \mathcal{T} . Since multiple nodes are associated with the same time period we denote by t_n the time period associated with node $n \in \mathcal{N}$. We also use p_n to denote the probability associated with visiting node n . All nodes, except for the root node ($t_n=0, p_n=1$), have a unique parent, $\Pi(n)$, and a recursive algorithm can be defined for determining p_n .

For the remainder of the paper we use the pair of subscripts, (*node, time period*) to denote state and decision variables associated with each node. For example \mathbf{u}_{n,t_n} will denote the vector of all decision variables for node n associated with time period t_n .

Each node n is born from its parent as a result of either

$$\tilde{\mathbf{I}}_{\text{RS}}(\mathbf{u}_{\Pi(n),t_{\Pi(n)}}) = 1 \text{ or } \tilde{\mathbf{I}}_{\text{RS}}(\mathbf{u}_{\Pi(n),t_{\Pi(n)}}) = 0.$$

For illustrative purposes, consider a node n born from $\tilde{\mathbf{I}}_{\text{RS}}(\mathbf{u}_{\Pi(n),t_{\Pi(n)}})=1$. In this case,

$$p_n = P_{\Pi(n)} P_{\Pi(n),t_{\Pi(n)}}^{(e_1 \cup e_2)}.$$

A depiction of scenario tree \mathcal{T} is shown in Fig. 1.

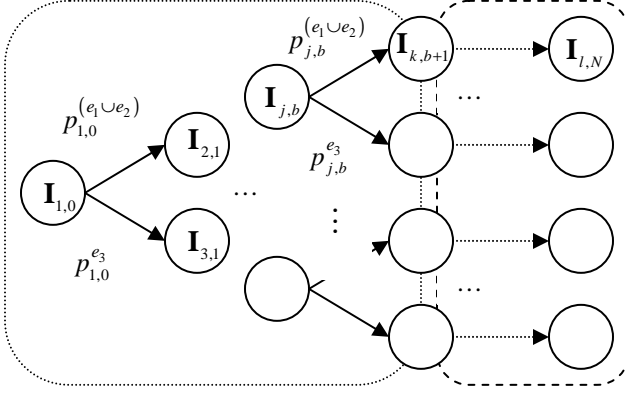


Fig. 1. Graphical depiction of MSP model. The look-ahead portion is indicated by the dotted line and the certainty equivalent by the dashed.

By considering the system dynamics as constraints, the SDP can now be approximated by linear programming problem in (16).

$$\min_{\mathbf{u}_{n,t_n} \in U(\mathbf{I}_{n,t_n})} \sum_{n \in N} E_{t_n} \left[g_{t_n}(\mathbf{I}_{n,t_n}, \mathbf{u}_{n,t_n}, \tilde{P}_{t_n}^E, \tilde{P}_{t_n}^R, t_n) \right]$$

Where for $t_n < N$,

$$E_{t_n} \left[g_{t_n}(\mathbf{I}_{n,t_n}, \mathbf{u}_{n,t_n}, \tilde{P}_{t_n}^E, \tilde{P}_{t_n}^R, t_n) \right] = cp_n x_{n,t_n}^\tau + p_n \sum_{\tau} \left\{ \begin{array}{l} E_{t_n} \left[\tilde{P}_{t_n}^E Q_{n,t_n}^E(\tau) \right] \\ \tilde{P}_{t_n}^{e_0} \\ + p_{n,t_n}^{e_1} E_{t_n} \left[\tilde{P}_{t_n}^E - \tilde{P}_{t_n}^R \right] Q_{n,t_n}^R(\tau) \\ \tilde{P}_{t_n}^{e_1} \\ + p_{n,t_n}^{e_2} E_{t_n} \left[\tilde{P}_{t_n}^E \right] Q_{n,t_n}^R(\tau) \\ \tilde{P}_{t_n}^{e_2} \end{array} \right\} \quad (16)$$

And for $t_n = N$,

$$g_N(\mathbf{I}_{n,N}, \mathbf{u}_{n,N}, \tilde{P}_N^E, \tilde{P}_N^R, N) = p_n \left(cx_{n,t_n=N}^{\tau=N} + \sum_{\tau > N} x_{n,t_n=N}^\tau \lambda_N^\tau \right)$$

Each node includes capacity constraints analogous to (8)-(10), non-negativity constraints, and system dynamic analogous to (5) and (7). However, the system dynamics with regards to the uncharged battery capacity are now explicitly modeled and thus (6) is reformulated in (17)-(18).

$$x_{n,t_n+1}^\tau = x_{n,t_n}^\tau + \hat{\Delta} x_{n,t_n}^\tau - [Q_{n,t_n}^E(\tau) + Q_{n,t_n}^R(\tau)] \Delta_{t_n} \quad n \in \mathcal{N}_a \quad (17)$$

$$x_{n,t_n+1}^\tau = x_{n,t_n}^\tau + \hat{\Delta} x_{n,t_n}^\tau - Q_{n,t_n}^E(\tau) \Delta_{t_n} \quad n \in \mathcal{N}_r \quad (18)$$

Note that we divide the set of nodes \mathcal{N} into two subsets \mathcal{N}_a and \mathcal{N}_r , where \mathcal{N}_a contains all nodes such that

$$\tilde{\mathbf{I}}_{\text{RS}}(\mathbf{u}_{\Pi(n),t_{\Pi(n)}}) = 1, \text{ and } \mathcal{N}_r \text{ contains all nodes such that}$$

$$\tilde{\mathbf{I}}_{\text{RS}}(\mathbf{u}_{\Pi(n),t_{\Pi(n)}}) = 0.$$

This formulation introduces equality constraints whose dual variables provide an estimate of λ_N^τ for $\tau > N$. The constraints corresponding to the initial distribution of $x_{1,0}^\tau$ for $\tau > N$ will have associated with them dual variables that represent the marginal cost of having one additional KWh of capacity for departure class τ at $t = 0$. Assuming that the modeled day is not drastically different from the subsequent day, these values should correspond to the marginal costs λ_N^τ . Computational experience has shown that these dual variables converge in one iteration except for extreme cases of distribution network congestion.

IV. COMPUTATIONAL EXPERIENCE

We employed a 24 time period horizon model with an equal number of explicit extension periods to incorporate departures scheduled outside of the modeled horizon. The first five time periods ($b=5$) comprise the look-ahead portion of the MSP horizon, while the remaining 19 time periods make up the certainty equivalent portion. The model begins at 12pm on Day 1 (i.e., $t = 0$), incorporates an estimated demand pattern, calculates charging decisions through 12pm (Day 2), and estimates uncharged energy with departure times from 1pm (Day 2) through 12pm (Day 3).

The LP solved contains approximately 70K state and decision variables, and an equal number of constraints. Data for the model inputs were derived from ERCOT (i.e., Texas) and CAISO (i.e., California), where wind farm generation is substantial and likely to develop at a rate amongst the fastest in the United States. The model was implemented in MATLAB codes, and the simulation platform was MATLAB 7.8.0 (R2009a). The implementation used MATLAB routines to run CPLEX 112 features in the MATLAB environment [15].

A. Model Inputs

Inputs were calibrated to represent a low voltage residential feeder servicing approximately fifty households. Using total number of household trips, trip type, trip length, and vehicle ownership data from the 2009 National Household Travel Survey [24], we developed an expected demand pattern for a neighborhood PHEV fleet. For simplicity, we defined five vehicle types based on their primary usage, as shown in Table I, and assumed a weekday-to-weekday scenario, meaning that the demand pattern was not expected to change significantly between Days 1, 2, and 3. Therefore, all PHEVs, except for the

“Extended Trip” type, have the same expected usage on both days.

TABLE I
EXPECTED PHEV DEMAND PATTERN

Vehicle Type	#	Arrival Times	Departure Times	Req. Ch. (KWh)
Work A	45	3pm – 6pm	6am – 9am	5.36
Work B	46	6pm – 9pm	6am – 9am	8.39
Non-Work A	12	7am – 10am	9am – 12pm	2
		10am – 1pm	12pm – 3pm	2
		1pm – 4pm	3pm – 6pm	2
		4pm – 7pm	6am – 9am	2
Non-Work B	11	7am – 10am	9am – 12pm	2
		10am – 1pm	12pm – 3pm	2
		1pm – 4pm	3pm – 6pm	2
Extended Trip	5	10am (Day 2)	6am (Day 3)	12

Probability distributions of hourly real-time wholesale market energy and regulation service clearing prices were estimated using ERCOT [5] and CAISO [1] data. We estimated ERCOT and CAISO energy and regulation service clearing price pdfs as $3\text{-}\sigma$ truncated normal distributions, with the parameters shown in Figs. 2 and 3. By properly integrating over the joint range spaces of these random variables, we computed the probability e_1 and e_2 for $t=0, \dots, N$.

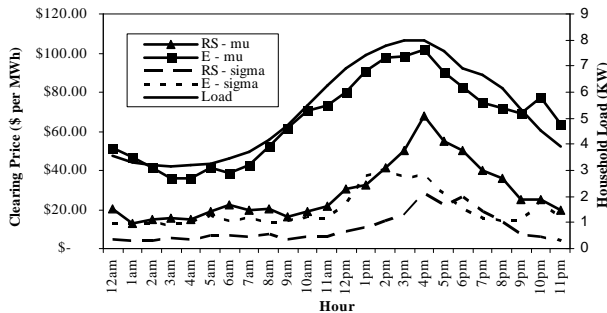


Fig. 2. ERCOT Pricing information and Non-PHEV load profile.

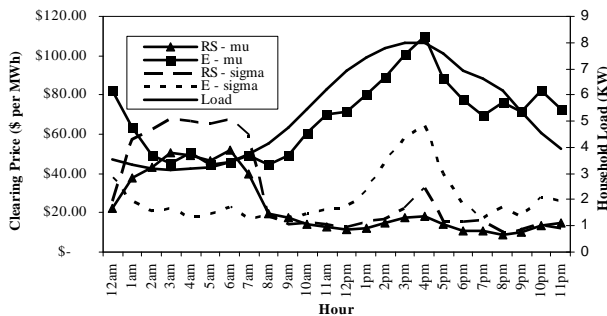


Fig. 3. CAISO Pricing information and Non-PHEV load profile.

Currently, ERCOT does not incorporate some of the more advanced market features found in other market operators (e.g., spot and day-ahead energy markets). Instead ERCOT uses the day-ahead load forecast to determine quantities of ancillary services, which can either be arranged through bilateral transactions or purchased in the day-ahead market. Subsequently, zonal balancing occurs by deploying balancing energy bids in real-time. For our analysis, we used day-ahead ancillary service data as a proxy for real-time

market reserve clearing prices. In addition, since ERCOT clears regulation service up and down separately, we summed the regulation service up and down clearing prices to estimate the clearing prices for an up-and-down band of regulation service capacity. Finally, we assumed our feeder location to be in the North Zone.

For CAISO, we used hour-ahead regulation service prices and aggregated hourly energy prices from CAISO’s real-time market. We assumed our feeder to be located in the NP-15 Region. It is interesting to note that CAISO’s maximum regulation service regulation price occurred in the early morning (i.e., between 12am and 8am) in 2008, while the peak energy price occurs at approximately 6pm. This shift occurred between 2007 and 2008; however, the reason for this shift is beyond the scope of this paper.

We modeled three distribution network congestion scenarios, corresponding to non-PHEV load during the peak hour of 80%, 90%, and 100% of the total feeder capacity. A typical summer residential consumption profile was drawn from data available from the Southern California Edison website [23].

B. Parameter Values

Uncharged capacity at the requested time of departure was penalized at \$0.75 per KWh (c), corresponding to a \$3 gallon of gasoline. A 2 KW charging rate (r) was assumed. Marginal distribution hourly losses in the distribution network were estimated for non-PHEV loads to range from 8% to 22%, and 1.08 to 1.22 multipliers were applied to wholesale market clearing prices in order to approximate retail prices. A transmission and distribution usage fee (\$0.04 per KWh) was computed by assuming that generation is responsible for 60% of end user energy costs.

The marginal cost of charging PHEVs with departure class outside of the modeled horizon, λ_N^τ for $\tau = N+1, \dots, 2N$, was first set equal to c for all departure classes. After an initial solution of the model, λ_N^τ was updated to equal the dual variables associated with the initial distribution of PHEVs scheduled to depart within the first 24 hours. To capture the impact of an infinite horizon, the model is resolved until λ_N^τ converges. The rate of convergence is a function of distribution line congestion, but did not require more than three iterations for the inputs used.

C. Computational Results

Each distribution network congestion scenario was run twice; *first* for smart-charging with regulation service, and *second* for smart-charging without regulation service. It was assumed that the ESCo will be able to negotiate a 50% reduction in the transmission and distribution usage fee in exchange for observing congestion constraints. Different discount rates can be easily explored. In addition, the cost of ‘dump-charging,’ namely the cost of charging immediately upon plugging-in, is calculated using time dependant electricity costs but no discount in the transmission and

distribution usage charges. Results are shown in Fig. 4. Decreasing the available distribution network capacity at peak from 20% to 10% did not impact the optimal charging decisions; however, decreasing to 0% resulted in a 6-9% increase in costs for both smart-charging strategies. Smart-charging without regulation service resulted in an average cost savings of 41% in ERCOT and 35% in CAISO when compared to dump-charging, while smart-charging with regulation service reduced costs by 50% in ERCOT and 56% in CAISO.

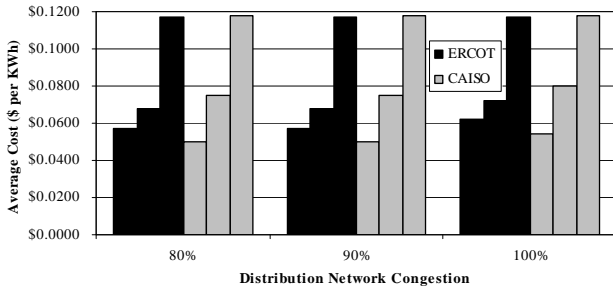


Fig. 4. Expected Cost by Charging Strategy: (i) smart-charging with regulation service, (ii) smart-charging without regulation service, and (iii) dump-charging, respectively.

Figs. 5 and 6 show the load profile for our ‘neighborhood’ under the different charging strategies for the ERCOT and CAISO model runs. If PHEV charging is not managed (i.e., dump-charging) then the peak energy consumption will increase and extend several additional hours. Smart-charging without regulation service will shift the charging to times of low distribution network congestion; however, charging will gravitate to a few hours resulting in a second peak in the load profile including the PHEV load. Smart-charging with regulation service offers the best option for load smoothing.

We finally discuss the implication of our computational results on the potential synergy of PHEV charging loads, wind generation intermittency and the often high wind potential during the night hours that pushes energy prices to very low levels [16]. Responding to high market clearing prices for regulation service and low clearing prices for energy, our proposed optimal PHEV battery charging methodology adapts to system wide costs addressing intermittency and high nighttime wind potential. Note first that we assume a household-outlet-compatible 2 KW (i.e., Level 1) charging rate. Our results show that in the ERCOT and CAISO model runs a minimum of 75% of the energy used to charge PHEV batteries correspond to regulation service. Assuming further that PHEVs will be plugged in 2/3 of the time and recognizing that (i) PHEVs should not provide regulation service whenever they are plugged-in, but only when there are proper market incentives; and (ii) local transmission capacity constraints may restrict PHEV regulation service provision during the day and early evening hours (see Fig. 3), a fact that we model by an additional factor of 60%, we conclude that each PHEV responding optimally to market signals can provide on the average

$$2 \text{ KW} \times \frac{2}{3} \times 0.75 \times 0.6 \approx 0.5 \text{ KW}$$

of regulation service.

The 0.5 KW or regulation service per PHEV is a conservative estimate based on no vehicle-to-grid capabilities, a practice that with today’s battery technology will severely decrease the useful life. With future technological breakthroughs and infrastructure that may allow higher charging rates (i.e., Levels 2 and 3) a 20 fold increase to 10 KW per PHEV may be possible [10].

If the Obama Administration achieves its target of 1 million PHEVs by 2015, KEMA et al. [9] estimate that 42,769 will ‘live’ in the ERCOT balancing area and 267,654 in CAISO. Based on our conservative estimate of 0.5 KW per PHEV, fleets of this size can provide 21 MW and 133 MW of regulation service, sufficient to support 420 MW and 2660 MW of installed wind capacity, respectively; using the Makarov et al. [12] estimate that wind farms will require additional regulation service equal to 5% of their installed capacity.

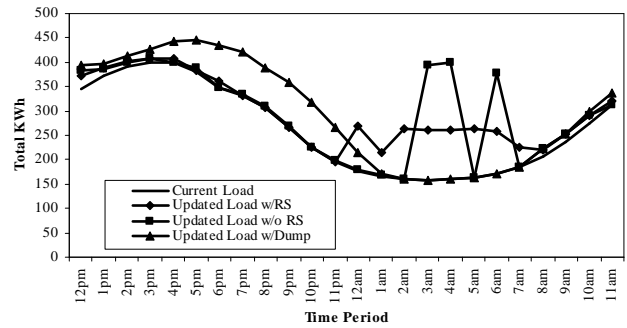


Fig. 5. ERCOT load profile by PHEV charging strategy.

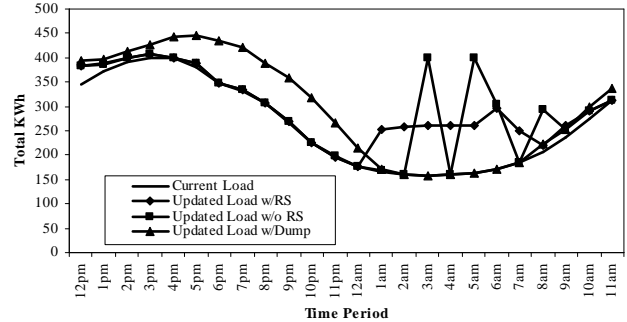


Fig. 6. CAISO load profile by PHEV charging strategy.

V. CONCLUSION AND FUTURE WORK

We developed a decision support tool for optimal PHEV market bidding policy. Computational results show that the resulting regulation service offered by PHEV charging loads can mitigate renewable generation intermittency costs. Moreover, optimal PHEV charging can render distribution network infrastructure resilient to new PHEV loads and deliver significant cost savings to PHEV operation.

In addition, the PHEV paradigm of a responsive load with linear dynamics generalizes to other important loads, for example, consider heating and cooling systems with the following parameters.

T_t^{inside}	The inside temperature at the beginning of decision period t .
$T_t^{outside}$	The forecasted outside temperature during decision period t .
T_t^{\min}, T_t^{\max}	Building occupant preferences during decision period t .
K_i	Known building constants for $i = 1, 2$.
$Q_t^{HC,E}$	Energy rate bid for decision period t . Intended for T_t^{inside} .
$Q_t^{HC,R}$	Regulation service capacity offered for decision period t . Intended for T_t^{inside} .
$Q_t^{HC,Capacity}$	Capacity of the HVAC system during decision period t .

The heating and cooling system dynamics and allowable control sets are perfectly analogous to PHEV dynamics and constraints as shown in (19)-(21). Other examples include dimmable lighting loads with a preferred lumen range as well as the load of smart appliances.

$$T_{t+1}^{inside} = T_t^{inside} - K_1(T_t^{inside} - T_t^{outside}) + K_2(Q_t^{HC,E} + Q_t^{HC,R}) \quad (19)$$

$$Q_t^{HC,E} + 2Q_t^{HC,R} \leq \min(\hat{C}_t^{\max}, Q_t^{HC,Capacity}) \quad (20)$$

$$T_t^{\min} \leq T_t^{inside} \leq T_t^{\max} \quad (21)$$

REFERENCES

- [1] California Independent System Operator (CAISO), Open Access Same-Time Information System (OASIS). [Online]. Available: <http://oasishis.caiso.com>.
- [2] M.C. Caramanis, J.M. Foster, "Management of Electric Vehicle Charging to Mitigate Renewable Generation Intermittency and Distribution Network Congestion," *48th IEEE CDC*, pp. 4717-4722, 2009.
- [3] M.C. Caramanis, J.M. Foster, E.A. Goldis, "Load Participation in Electricity Markets: Day-Ahead and Hour-Ahead Market Coupling with Wholesale/Transmission and Retail/Distribution Cost and Congestion Modeling," *First IEEE Conference on Smart Grid Communications*, Regular Session, Oct. 2010.
- [4] T. Dominguez, M. De La Torre, G. Juberias, E. Prieto, A. Cordoba, "Wind Generation Issues in Spain and Real-Time Production Control" CIGRE Conference, Zagreb, 2007.
- [5] Energy Reliability Council of Texas (ERCOT), Day-Ahead Ancillary Market Clearing Prices for Capacity Archives, Balancing Energy Services Market Clearing Prices for Energy Annual Reports Archives, 2007-2009. [Online]. Available: <http://www.ercot.com>.
- [6] ERCOT Reliability and Operations Subcommittee, "Effects of Wind on Frequency," June 13, 2007, Report.
- [7] H. Holttinen et al., "Design and Operation of Power Systems with Large Amounts of Wind Power: State-of-the-Art Report," IEA, Oct. 2007.
- [8] K. Huang and S. Ahmed, "The Value of Multistage Stochastic Programming in Capacity Planning Under Uncertainty," *Oper. Research*, vol. 57(4), pp. 893-904, Aug. 2009.
- [9] KEMA and IRC, "Assessment of Plug-in Electric Vehicle Integration with ISO/RTO Systems," Produced for the ISO/RTO Council in conjunction with Taratec, Mar. 2010, 65 pp.
- [10] W. Kempton, J. Tomic, "Vehicle-to-Grid Power Implementation: From Stabilizing the Grid to Supporting Large-Scale Renewable Energy," *J. Power Sources*, vol. 144, pp. 268-279, 2005.
- [11] F. Li, N. P. Padhy, J. Wang, "Cost-Benefit Reflective Distribution Charging Methodology," *IEEE Trans. on PS*, vol. 23, no. 1, 2008.
- [12] Y.V. Makarov, C. Loutan, J. Ma, and P. de Mello, "Operational Impacts of Wind Generation on California Power Systems," *IEEE Trans. on PS*, vol. 24, no. 2, pp. 1039 - 1050, May 2009.
- [13] M. Milligan and B. Kirby, "Analysis of Sub-Hourly Ramping Impacts of Wind Energy and Balancing Area Size: Preprint," presented at the WindPower 2008, Houston, TX, June 2008. [Online]. Available: <http://www.nrel.gov/wind/pdfs/43434.pdf>.
- [14] M. Milligan and K. Porter, "Determining the Capacity Value of Wind: An Updated Survey of Method and Implementation," presented at the WindPower 2008, Houston, TX, June 2008, preprint. [Online]. Available: <http://www.nrel.gov/docs/fy08osti/43433.pdf>.
- [15] D.R. Musicant, MATLAB/CPLEX MEX-Files, Computer Science Department, University of Wisconsin, Madison, 2000. [Online]. <http://cs.carleton.edu/faculty/dmusicant/cplex/index.html>.
- [16] A.L. Ott, "Demand Response in the PJM Synchronized Reserve Market: Experience and Prospects," *Presentation at Disrupting the Status Quo in Electric Energy Management*, Boston University, May 2009.
- [17] L. A. Ott, "Implementation of Demand Response in the PJM Synchronized Reserve Market," 2008 CIGRE Paris Session and Technical Exhibition, Paris, France, August 24-29, 2008.
- [18] R. Piwko et al., "Intermittency Analysis Project: Appendix B Impact of Intermittent Generation on Operation of California Power Grid, California Energy Commission, PIER Renewable Energy Technologies Program. CEC-500-2007-081-APB, Jul. 2007. [Online]. Available: <http://www.energy.ca.gov/2007publications/CEC-500-2007-081/CEC-500-2007-081-APB.PDF>.
- [19] PJM, "White Paper on Integrating Demand and Response into the PJM Ancillary Service Markets," Feb. 2005.
- [20] A. Ruszcynski and A. Shapiro, *Stochastic Programming. Handbooks in Operations Research and Management Science*, v. 10, Elsevier 2003.
- [21] K.J. Singh, A.B. Philpott, R.K. Wood, "Dantzig-Wolfe Decomposition for Solving Multi-Stage Stochastic Capacity-Planning Problems," Working paper, Electric Power Optimization Centre, University of Auckland, New Zealand, 2005.
- [22] J.C. Smith, M.R. Milligan, E.A. DeMeo, and B. Parsons, "Utility Wind Integration and Operating Impact State of the Art," *IEEE Trans. on PS*, vol. 22, no. 3, pp. 900 - 908, Aug. 2007.
- [23] Southern California Edison, Regulatory Information - SCE Load Profiles, 2009. [Online]. Available: <http://www.sce.com>.
- [24] U.S. Department of Transportation, Federal Highway Administration, National Household Travel Survey (NHTS) Data, 2009. [Online]. Available: <http://nhts.ornl.gov/publications.shtm>.
- [25] J. Zhang, J.D. Fuller, and S. Elhedhli, "A Stochastic Programming Model for a Day-Ahead Electricity Market with Real-Time Reserve Shortage Pricing," *IEEE Trans. on PS*, vol. 25, no. 2, pp. 703-713, May 2010.